Nuclear Instruments and Methods in Physics Research B47 (1990) 118–125
North-Holland

THE EFFECTS OF SURFACE ROUGHNESS CHARACTERIZED BY FRACTAL GEOMETRY ON SPUTTERING

David N. RUZIC

Department of Nuclear Engineering, University of Illinois, 103 South Goodwin Ave., Urbana, Illinois 61801, USA

Received 27 July 1989 and in revised form 7 November 1989

Fractal geometry has been added to the binary-collision TRIM computer code to simulate realistic atomic-scale surface roughness. This inclusion significantly affects TRIM sputtering yields and reflection coefficients at low energies (10s to 100s of eV) and non-normal angles of incidence. Results are shown and favorably compared to experiments for H and C sputtering of C as a function of angle, energy and fractal dimension. Energy and angular distributions of the sputtered and reflected particles as a function of fractal dimension are also shown.

1. Introduction

The sputtering yield, Y, is the number of surface atoms expelled per incoming particle. Its value is critical for many applications. In controlled fusion research the choice of plasma-facing materials is almost completely determined by their sputtering yield as a function of energy. If the yield is too high, the material will erode, cooling the plasma below the temperatures needed for fusion and shortening the lifetime of the divertor, limiter or first-wall. The angular and energy distribution of the sputtered material is important as well. Since virtually all sputtered atoms are electrically neutral, they will cross the magnetic flux surfaces. Therefore, the distributions determine the source term for the impurities in the main plasma [1] and the redeposition on the plasma-facing surfaces [2].

In plasma processing, sputtering is an important phenomena as well. Many metalizations are accomplished by sputtering a magnetron target with plasma ions. Semiconductor and insulating material can also be deposited through sputtering. Again the energy and angular distribution of the sputtered material is crucial to any detailed modelling or understanding of the deposited material [3].

The energy range of the vast majority of incident particles for both fusion and plasma processing is 10s to 100s of eV. When a surface is struck by such a particle, an isotropic collision cascade does not materialize. Instead some atoms, often referred to as primary knock-ons, may gain a substantial amount of the incident atom's energy through the collision. They in turn can sputter or strike other atoms transferring momentum yet again [4,5]. Further, when considering energies on this scale the geometric features of the surface become very important. The range of the incident particle in the solid may be comparable to the atomic-scale roughness.

The computer code TRIM [6–8] uses a binary collision model and follows the incident particle and all of its cascade members until they sputter or their energy becomes too low to escape the surface potential. However, the surface model in TRIM is primarily planar and variations in surface roughness have not been treated. This paper uses statistical and geometrical aspects of fractal geometry [9,10] to simulate surface roughness as a function of fractal dimension in the TRIM computer code. The cases described here all use carbon as the target. It has been shown [11] that graphites have measurable atomic fractal characteristics: Vulcan 3G graphite has a fractal dimension, D, of 2.07 ± 0.01; carbon black has $D = 2.25 \pm 0.09$. Previous work [12] describes incident atom reflection and the modifications to TRIM in more detail. This paper shows fractal TRIM sputtering results for H on C and C on C and compares the results of the simulations to planar TRIM results [13] and to recent experiments [14,15].

2. Fractal modeling

Fractal TRIM differs from the standard planar TRIM in two ways. The first is the initial placement of the projectile with respect to the surface. Planar TRIM uses a surface model which places the incident particle at a random depth based on the chance of encountering a surface atom within concentric cylinders whose axes align with the particles path [7]. This gives the surface a roughness with a characteristic depth of the order of the incident atoms mean free path in the solid. Fractal TRIM places the incident particle just inside a fractal

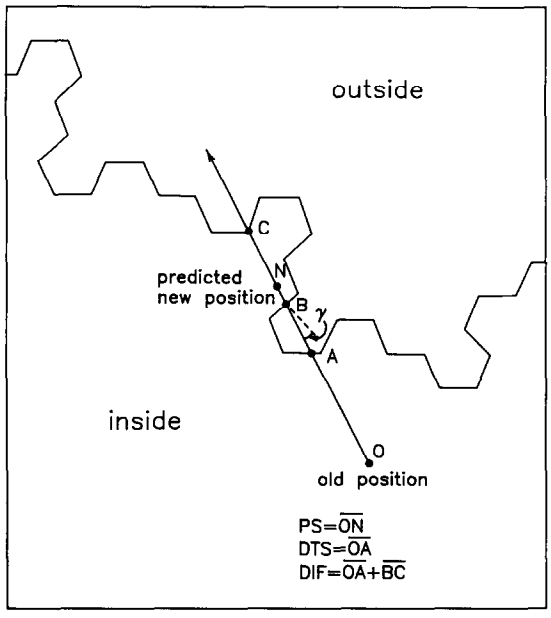

Fig. 1. A drawing of the surface geometry and one portion of a particle's flight path. PS is the path step, DTS is the distance to the surface, and DIF is the distance in the fractal.

intersection surface. This position is determined by starting the incident particle above the center of the fractal construct within a random vertical range and then calculating the intersection point of the particle's trajectory with the surface. In both planar and fractal TRIM the incident angle is refracted by the surface potential.

The second difference between planar and fractal TRIM is the exit condition. In both codes the paths of the incident and cascade particles are determined and tracked. At each step positions are checked to determine whether a particle has exited the surface. In planar TRIM the surface model inquires whether the particle has reached above a fixed plane. If so, the surface model is used to determine if another atom will be encountered or not. In fractal TRIM the same surface routine is used, but the inquiry point is not a fixed plane. It is a fractal whose minimum extent is fixed by the closest interatomic spacing of the target and whose maximum extent is determined by the overall range of the projectiles.

The fractal boundary is implemented as shown in fig. 1. At each step for the incident or cascade particles the new position that TRIM would predict for the particle is calculated (point N). The distance between the old position (point O) and the new predicted position is called the path step, PS. Then the distance to the surface (DTS) along the line from the old position to the new position (line segment from point O to point A) is determined. If PS is less than DTS, TRIM continues with no modifications. If PS is greater then DTS the particle will cross at least one surface. Now a new quantity is calculated, the distance in the fractal (DIF). In fig. 1 an example is shown where DIF equals DTS plus only one additional segment. There are many trajectories where several segments must be added to compute DIF. If PS is also greater than DIF, the particle indeed escapes – provided its perpendicular energy is great enough to overcome the surface potential as in planar TRIM.

If PS is less than DIF, the particle's new position will lie within the solid once again. It would be unrealistic however to locate the particle at the particular outcropping along its current trajectory. TRIM is a three dimensional simulation and the fractal surface represented in fig. 1 is just the intersection of the scattering plane with the fractal surface. The next collision will send the particle out of that scattering plane and into a new one.

Here is where the rotational self-similarity of fractals is used. The angle at which the projectile strikes the first fractal surface crossed (γ) is recorded along with the particle's energy at that point. Then a new simulation is restarted using γ as the incident angle and the projectile's current energy as the incident energy. Note that if TRIM is following a member of the collision cascade a target atom may have to be treated as an incident particle. Once the new simulation (and any simulations it starts) is finished, the program picks up the old cascade where it left off.

Particles that are restarted in this manner were likely to have been near a surface. Nearness to some surface is preserved in the restarted simulation because of the initial placement routine. Restarted particles were also likely to have a velocity directed outward from the surface. This is not necessarily preserved. However, molecular dynamic simulations of atoms moving just above an atomically rough surface do show a bending of their paths toward the normal of local surface features [16]. The restart routine effectively encompasses this effect.

If a particle can geometrically leave the surface it may not be allowed to do so due to the surface potential. To overcome the surface potential the component of the kinetic energy that is perpendicular to the surface must exceed the surface binding energy. Those atoms with insufficient energy will bounce. In planar TRIM these bounces are specularly reflected and placed at a depth one mean free path lower than their collision point. In fractal TRIM, that point could conceivably lie on the other side of the surface. Instead, the bounces are given some variation about a specular reflection angle and repositioned at their previous position with an appropriately decremented energy. These previous positions are typically closer to the surface than the new position given the atoms by planar TRIM.

If the energy is large enough to leave, the surface potential will still refract the particle and subtract a portion of its energy. This simulation treats both the initial entering and final exiting refraction with respect to the overall surface plane. However, internal jumps from one surface feature to the next effectively treat refraction with respect to the local surface normal. The effect of this assumption is discussed further with respect to fig. 7 in the results section.

Fractal TRIM can be run with a fractal surface with a dimension of 2.000. This is not equivalent to planar TRIM, but due only to the varying initial depth built into the planar TRIM initial placement routine. If planar TRIM is forced to have starting positions that lie precisely on the surface plane, as fractal TRIM with $D = 2.00$ would give, the results are identical even though all the fractal intersection routines are calculated at each step.

To highlight the important difference in surface models, and to plot the planar TRIM results as a function of D accurately, some equivalent fractal dimension must be calculated for the planar TRIM surface model. This equivalent dimension will vary with incident angle and energy, and the target's surface binding energy. For the case of C incident on C at 100 eV with a surface binding energy of 7.4 eV [17], the equivalent fractal dimensions were calculated to be $D = 2.00$, 2.05, 2.08, 2.07 and 2.06 for $\alpha = 0°$, 20°, 40°, 60° and 75°. Details of the calculation are shown in the appendix.

3. Results

Fractal TRIM takes about seven times longer to run than planar TRIM. Factors of 2 improvement are expected with vectorization of the code and streamlining of the geometric routines. The data presented here were computed on a Cray XMP-48. A typical run of 1000 flights took approximately 1 to 4 min depending upon the masses and incident energy. Standard statistical errors in the data are generally less than 5 to 10%. The error can be calculated precisely for any particular data point by taking the square root of the number of flight conclusions represented by that point. Some representative error bars on the simulation data are shown in the figures. Error bars for the cited experimental data were not shown in refs. [14] and [15].

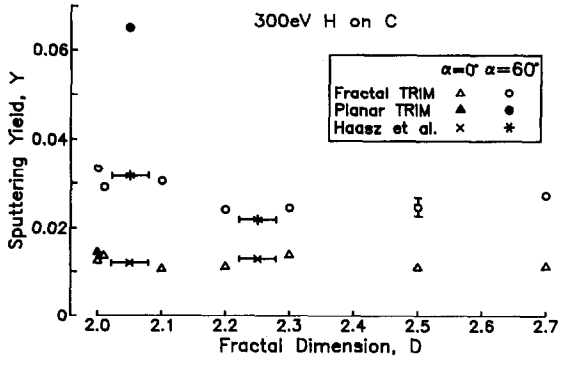

Fig. 2. Sputtering yield of 300 eV H on C as a function of fractal dimension, D. The D of the experimental points of Haasz et al. [14] is based on work of Avnir et al. [11].

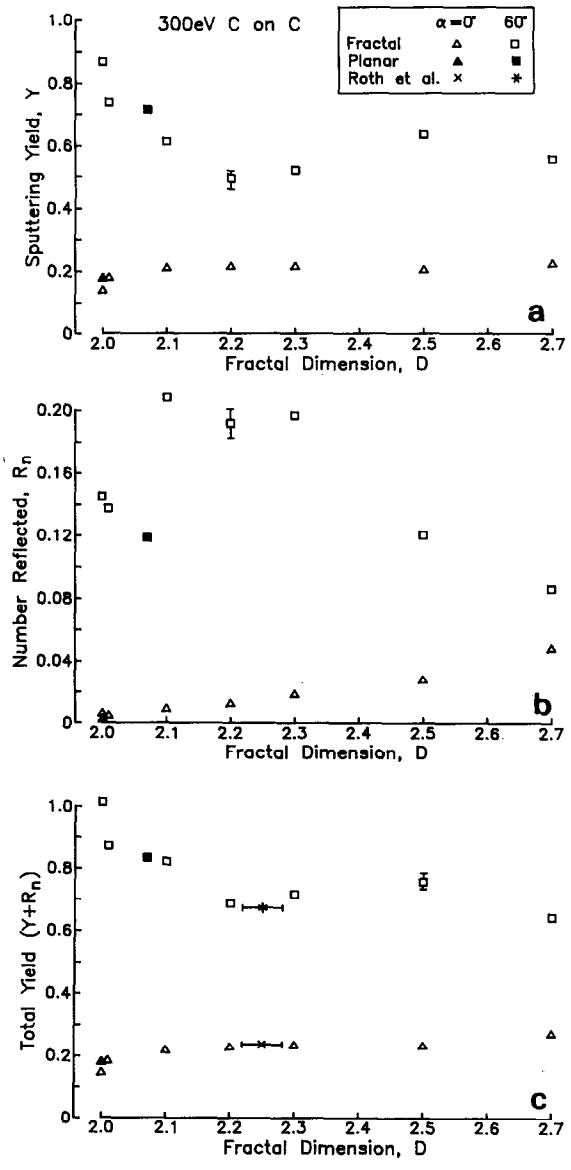

Fig. 3. (a) Sputtering yield of target atoms, (b) normalized number of incident atoms reflected, and (c) total self-sputtering yield for 300 eV C on C as a function of fractal dimension, D. The D of the experimental points of Roth et al. [15] is based on work of Avnir et al. [11].

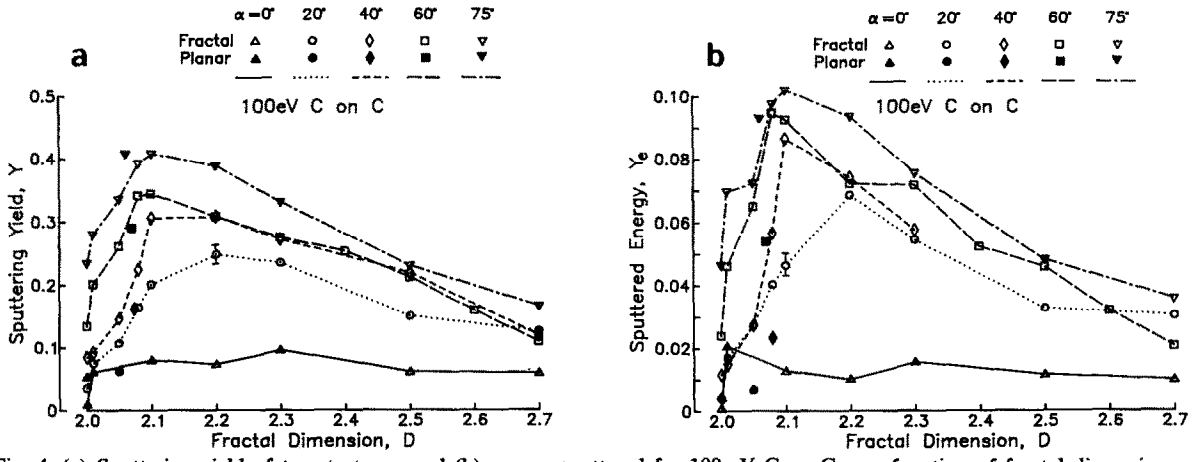

Fig. 4. (a) Sputtering yield of target atoms, and (b) energy sputtered for 100 eV C on C as a function of fractal dimension and incident angle.

Fig. 2 shows the sputtering yield as a function of fractal dimension for 300 eV H on C at incident angles of 0° (normal) and 60°. Each run consisted of 5000 flights. The fractal TRIM results are more than a factor of two lower than the planar TRIM results for the higher angles of incidence. As the surface roughness increases, there is a decrease in the sputtering yield. This behavior is also seen in other cases where the incident projectile is much lighter than the target.

Also shown in fig. 2 are experimental results [14] for two differing types of graphite: a smoother highly oriented pyrolytic graphite and a rougher isotropic fine-grain graphite. The fractal dimension has not been measured for these materials. Their placement as a function of D is based on the experimental measurements of Avnir et al. [11]. Regardless of the specific placement, the rougher material showed a lower sputtering yield at 60° and fitted the fractal TRIM calculation more closely then the planar TRIM calculation.

When the projectile and the target are the same, there is no experimental way based on a single event to distinguish between sputtering and reflection. Computer simulations, however, track the incident and target atoms independently. Figs. 3a and b show these individual components of the self-sputtering yield for 300 eV C on C at incident angles of 0° and 60°. Fig. 3c sums the contributions and compares the total sputtering yield to experimental results. Each run consisted of 2000 flights. Again the assignment of a fractal dimension to the not highly oriented (atomically rough) pyrolytic graphite used by Roth et al. [15] is based upon the measurements of Avnir et al. [11].

At lower energies, the effects of surface roughness are more pronounced. Figs. 4a and b show the yield of

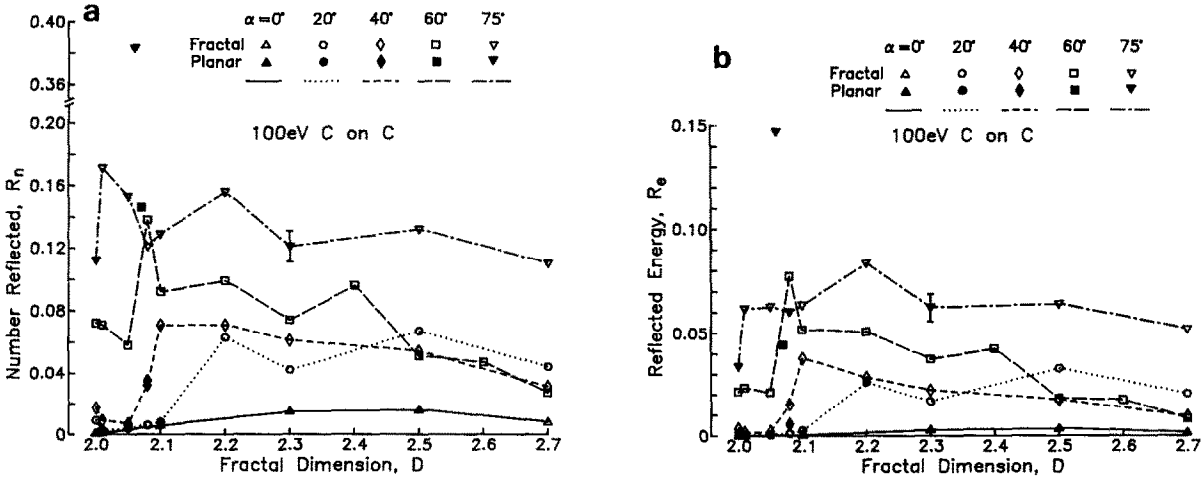

Fig. 5. (a) Normalized number of incident atoms reflected, and (b) reflected incident energy for 100 eV C on C as a function of fractal dimension and incident angle.

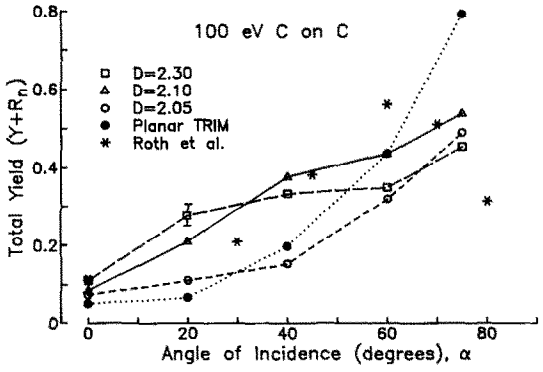

Fig. 6. Total sputtering yield for 100 eV C on C as a function of angle for a variety of fractal dimensions compared to experimental points of Roth et al. [15]. The experimental points at 70° and 80° may be higher than shown due to the measurement method used.

sputtered target atoms and the energy yield of sputtered target atoms as a function of fractal dimension and angle of incidence. Each run consisted of 1000 flights. Note that for most roughnesses the yield is considerably lower at higher angles of incidence than that predicted from planar TRIM. Note also the rapid increase in sputtering yield as soon as any roughness is added. If a surface is perfectly flat, the first target atom encountered must have a component of its initial new velocity directed toward the surface. With even a small degree of topographic variation an initial knock-on atom may have a velocity component away from the surface. However, if the surface becomes too convoluted these initially sputtered atoms may run into surface features on their way out. This trend is clearly seen in the data. As the angle of incidence increases the degree of roughness required to begin lowering the sputtering yield decreases.

Figs. 5a and b show the number of reflected incident atoms and the amount of reflected incident energy for 100 eV C on C as a function of fractal dimension and angle. These results come from the same computer runs as the data shown in fig. 4. Note the broken vertical scale in fig. 5a. Planar TRIM predicts a much higher reflection coefficient at grazing angles of incidence than fractal TRIM.

Fig. 6 compares the total sputtering yield for 100 eV C on C as a function of D to experimental results of

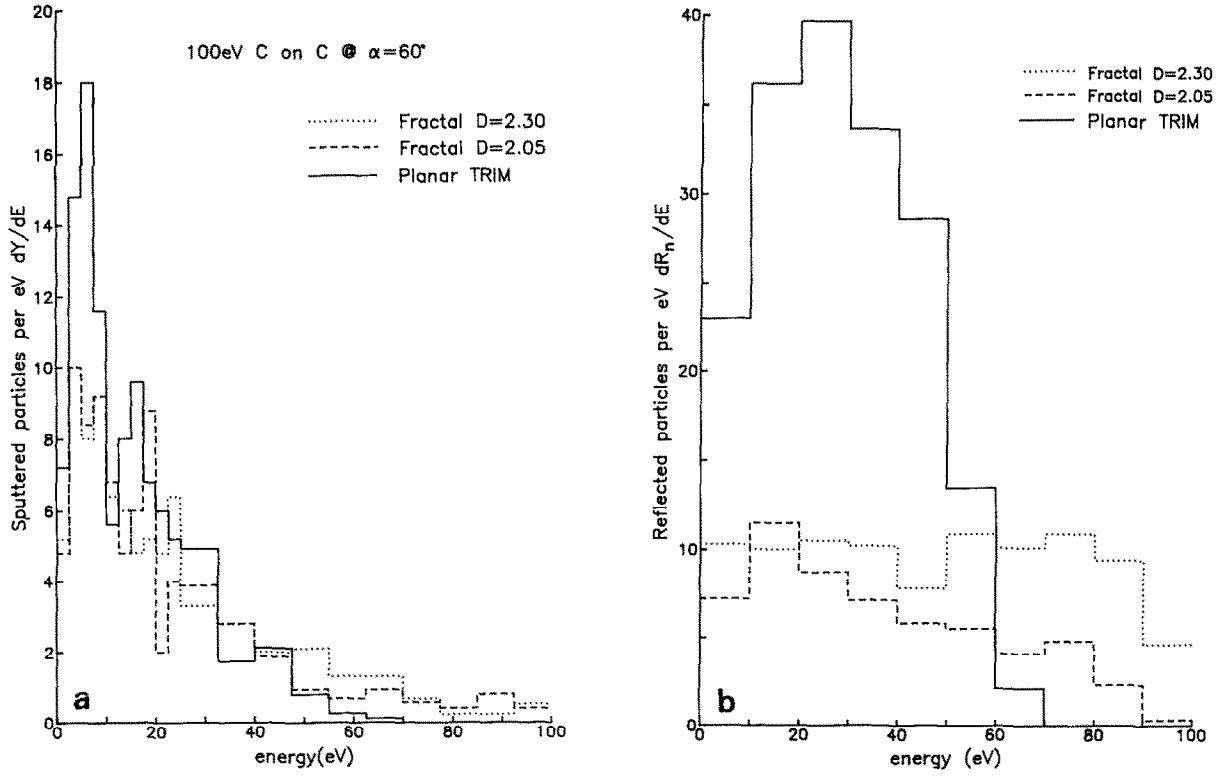

Fig. 7. (a) Differential sputtered target particle energy distributions, and (b) differential reflected incident particle energy distributions for 100 eV C on C at an incident angle of 60° from normal. Particles with very large reflected energies are peculiar results of the simulation and are discussed in the text.

Roth et al. [15]. The experimental results at higher angles of incidence (70° and 80°) may not completely account for reflected carbon atoms and are therefore expected to be higher than shown. The fractal results for $D = 2.1$ or 2.3 simulate the results more closely than the planar TRIM data.

The addition of atomic surface roughness also changes the energy distribution of the sputtered and reflected flux. More high-energy particles are seen. Figs. 7a and b show the sputtered target and reflected projectile energy distributions of 100 eV C on C at an incident angle of 60°. The runs for fig. 7a consisted of 1000 flights while the run for fig. 7b did not calculate sputtering and consisted of 10000 flights. In fig. 7a, some target atoms are shown escaping with nearly all of their incident energy. In fig. 7b, some atoms are seen to reflect with nearly all of their incident energy. These results come exclusively from events where the projectile skips off or through surface protrusions. In accordance with the restart model these particles' refractions are effectively taken with respect to the local surface normals during the non-end points of their flights, thereby allowing such paths. No strict binary collision has occurred. Therefore they are not required to lose the classical minimum energy which leads to the sharp cut-off in the planar TRIM results. The validity of such events is not experimentally verified, but still points to higher average energies of sputtered and reflected flux than predicted by planar TRIM.

Figs. 8a and b show the polar angular distributions of the sputtered target atoms and reflected projectile atoms for 100 eV C on C at an incident angle of 75° as a function of fractal dimension. The runs for fig. 8 consisted of 1000 flights each. Both the reflected and sputtered distributions of planar TRIM show a typical specular reflection pattern. As the roughness is increased the distributions become cosine in nature. The atoms ejected normally from the surface ($\cos\beta = 1.0$) in the $D = 2.20$ case are predominantly those with low energy. Due to the surface potential, particles with low energy can only be emitted if their trajectory is almost normal to the surface. These particles are also likely to bounce at least once before escaping. Since planar TRIM artificially lowers these atom's positions upon bouncing it is not surprising to see few of them emitted.

4. Discussion

Fractal geometry allows atomic surface roughness to be added to computer simulations in a realistic manner. The results of incorporating a fractal surface model into TRIM correct some simulation deficiencies at low en-

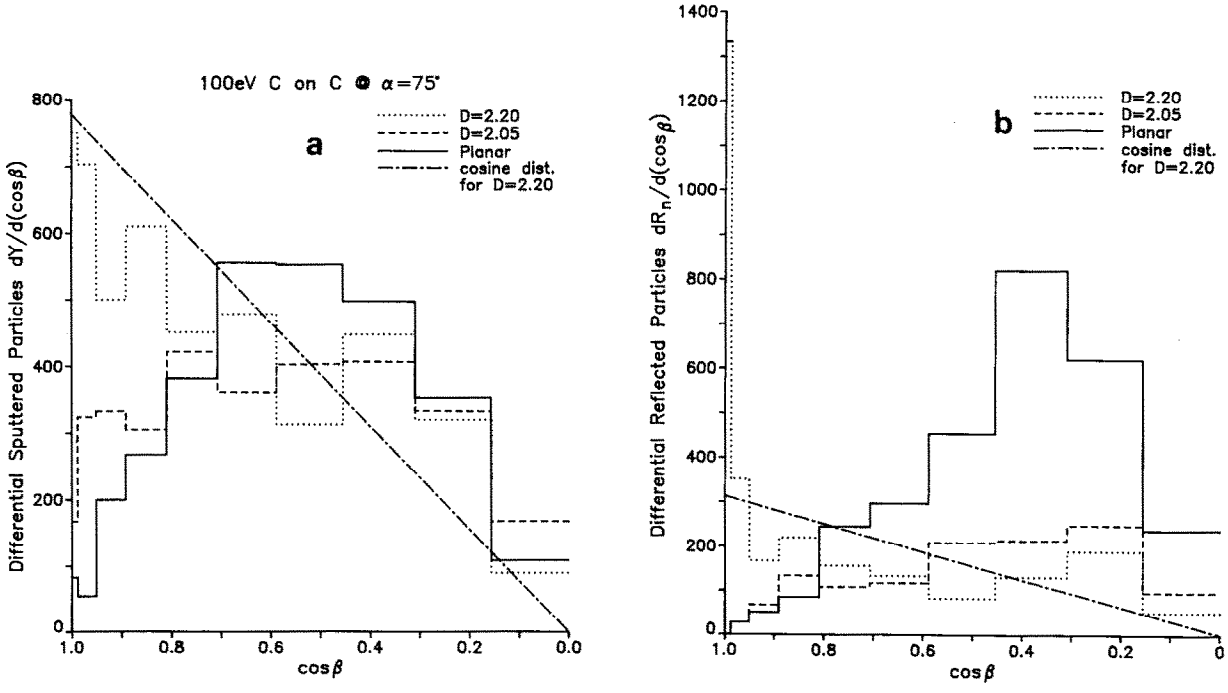

Fig. 8. (a) Differential sputtered target particle angular distributions, and (b) differential reflected incident particle angular distributions for 100 eV C on C at an incident angle of 75° from normal. A cosine distribution for the $D = 2.20$ case is also shown.

ergy and grazing angles of incidence and improve agreement with experimental data.

The implications of potentially more accurate simulations of sputtering are quite important to material choices for future fusion energy devices. Materials with self-sputtering yields of unity at energies of interest must be absolutely avoided. However, to reap the full benefit of fractal TRIM, BET-type [18] measurements of surface roughness utilizing a variety of adsorbent sizes should be carried out on samples from present fusion research devices to determine their atomic fractal character.

Macroscopic roughness, that is, the microsized pores, hills and valleys visible in typical SEMs, is not addressed by the simulations presented here. Future work will address roughness on differing scales.

I wish to thank and acknowledge the Max Planck Institut für Plasmaphysik for permission to use the TRIM code and Dr. Wolfgang Eckstein for many illuminating discussions. Computer time was granted by the National Center for Super Computing Applications at the University of Illinois, and funding was provided by the Presidential Young Investigator Program of the US National Science Foundation (CBT-84-51599).

Appendix

An incident particle is refracted toward the surface normal upon entering a surface by the surface potential according to:

$$\sin^2 \alpha' = \frac{E_0}{E_0 + E_{sb}} \sin^2 \alpha,$$

where α is the initial incident angle with respect to the normal, α' is the new angle, E_0 is the incident energy and E_{sb} is the surface binding energy.

The surface model [7] of the TRIM code produces a probability distribution for the depth of the first atom encountered. Two simplifications are required to reduce the distribution to a tractable analytic form: the random spread of impact parameters is linear instead of logarithmic, and only the first concentric cylinder about the flight path is needed to find an impacting atom. With these assumptions, the probability distribution can be approximated by the surface shown in bold in fig. 9. P_{max} is related to the atomic density of the target material, but is ultimately not needed to calculate the fractal characteristic.

The probability distribution can be treated as a fractal generator and a characteristic fractal dimension, D, can be found. The D of a fractal generator is the log of the distance along the fractal surface divided by the log of the distance along the plane. Therefore, following fig. 9,

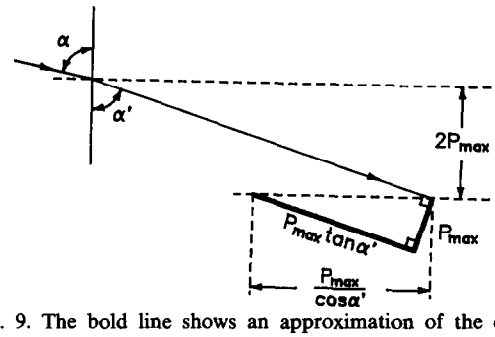

Fig. 9. The bold line shows an approximation of the depth distribution of initially encountered atoms in the TRIM surface model [7].

$$D = \frac{\log\left(R \frac{P_{max} \tan \alpha' + P_{max}}{P_{max}/\cos \alpha'} \right)}{\log (R)},$$

$$= \frac{\log(R(\cos \alpha' + \sin \alpha'))}{\log (R)},$$

where R is taken as the same overall extent of the fractal simulation – the distance at which 99% of the paths do not escape. For the runs shown here, $R = 80$ Å.

References

[1] C.S. Pitcher, P.C. Stangeby, D.H.J. Goodall, G.F. Matthews and G.M. McCracken, J. Nucl. Mater. 162–164 (1989) 337.
[2] J.N. Brooks, D.K. Brice, A.B. DeWald and R.T. McGrath, J. Nucl. Mater. 162–164 (1989) 363.
[3] J.J. Cuomo, S.M. Rossnagel and H.R. Kaufman (eds.), The Handbook of Ion Beam Processing Technology (Noyes, Park Ridge, New Jersey, USA, 1989).
[4] H.H. Andersen, in: Sputtering by Particle Bombardment, ed. R. Behrisch (Springer, Berlin, 1981) chap. 4.
[5] D.N. Ruzic, in: Plasma-Based Processes, eds. S.M. Rossnagel, J.J. Cuomo and W.D. Westwood (Noyes, Park Ridge, New Jersey, USA, 1989) chap. 3.
[6] J.P. Biersack and L.G. Haggmark, Nucl. Instr. and Meth. 174 (1980) 257.
[7] J.P. Biersack and W. Eckstein, Appl. Phys. A34 (1984) 73.
[8] W. Eckstein and D.B. Heifetz, J. Nucl. Mater. 145–147 (1987) 332.
[9] B.B. Mandelbrot, The Fractal Geometry of Nature (Freeman, San Fransisco, 1982).
[10] J. Feder, Fractals (Plenum, New York, 1988).
[11] D. Avnir, D. Farin and P. Pfeifer, J. Chem. Phys. 79 (1983) 3566.
[12] D.N. Ruzic and H.K. Chiu, J. Nucl. Mater. 162–164 (1989) 904.
[13] W. Eckstein and J.P. Biersack, Z. Phys. B63 (1986) 109.

[14] A.A. Haasz, J.W. Davis and C.H. Wu, J. Nucl. Mater. 162–164 (1989) 915.
[15] J. Roth, J. Bohdansky and W. Ottenberger, J. Nucl. Mater. 165 (1989) 193.
[16] D.N. Ruzic, H.K. Chiu, C. Hoyer, and R. Idasak, Molecular Dynamics on a Rough Surface, a scientific video, published and available from the National Center for Supercomputing Applications, Scientific Media Services, University of Illinois, 605 E. Springfield Ave., Champaign IL USA 61820 (1990).
[17] R. Hultgren, J.P. Desai, D.T. Hawkins, M. Gleiser, K.K. Kelley and D.D. Wagman, Selected Values of the Thermodynamic Properties of the Elements (Am. Soc. Metals, Metals Park, Ohio, USA, 1973).
[18] S. Brunaner, P.H. Emmett and E. Teller, J. Am. Chem. Soc. 60 (1938) 309.